

whereas the effect of dissipative torques is to reduce the angle between the axes.

On short timescales it is appropriate to consider the core to be an inviscid fluid constrained to move within the ellipsoidal region bounded by the rigid mantle [43–45]. The inertial coupling provided by this mechanism is effective whenever the ellipticity of the container exceeds the ratio of the precessional to rotational rates. If the mantle were actually rigid, or even elastic [46,47], this would be an extremely effective type of coupling. However, on sufficiently long timescales, the mantle will deform viscously and can accommodate the motions of the core fluid [48]. The inertial coupling torque exerted by the core on the mantle will have the form

$$T_i = k_i[\chi_m \times \chi_c] \quad (9)$$

A fundamentally different type of coupling is provided by electromagnetic or viscous torques [49–51]. The dissipative coupling torque exerted by the core on the mantle will have the form

$$T_d = k_d[\chi_m \times \chi_c] \quad (10)$$

This type of coupling is likely to be most important on longer timescales. In each case, the mantle exerts an equal and opposite torque on the core. The response of the coupled core-mantle system to orbital forcing is given by [52–54]

$$\begin{aligned} ds_m/dt &= \alpha_m(n \cdot s_m)(s_m \times n) - \beta_m(s_m - s_c) - \gamma_m(s_m \times s_c) \\ ds_c/dt &= \alpha_c(n \cdot s_c)(s_c \times n) + \beta_c(s_m - s_c) + \gamma_c(s_m \times s_c) \end{aligned} \quad (11)$$

where α_m is similar to α above, except that only mantle moments A_m and C_m are included, and

$$\begin{aligned} \beta_m &= k_d/C_m \nu \\ \gamma_m &= k_i/C_m \nu^2 \end{aligned} \quad (12)$$

where ν is the mean rotation rate.

References: [1] Hays T. D. et al. (1976) *Science*, 194, 1121–1132. [2] Berger A. L. et al. (1984) *Milankovitch and Climate*, Reidel, Dordrecht, 895 pp. [3] Milani A. (1988) In *Long-term Dynamical Behavior of Natural and Artificial N-body Systems* (A. E. Roy, ed.), 73–108, Reidel, Boston. [4] Laskar J. (1988) *Astron. Astrophys.*, 198, 341–362. [5] Richardson D. L. and Walker C. F. (1989) *J. Astron. Sci.*, 37, 159–182. [6] Quinn T. R. et al. (1991) *Astron. J.*, 101, 2287–2305. [7] Laskar J. (1990) *Icarus*, 88, 266–291. [8] Kinoshita H. (1977) *Celest. Mech.*, 15, 215–241. [9] Williams K. G. et al. (1991) *Astron. Astrophys.*, 241, L9–L12. [10] Bills B. G. (1989) *GRL*, 16, 385–388. [11] Bills B. G. (1990) *JGR*, 95, 14137–14153. [12] Miskovic V. V. (1931) *Glas. Spr. Kraljevske Acad.*, 143. [13] Sharaf S. G. and Boudnikova N. A. (1967) *Bull. Inst. Theor. Astron.*, 11,

231–261. [14] Vernekar A. D. (1972) *Meteor. Mon.*, 12, 1–22. [15] Vernekar A. D. (1977) In *The Solar Output and Its Variations* (O. R. White, ed.), 117–130, Univ. of Colorado. [16] Ward W. R. (1974) *JGR*, 79, 3375–3381. [17] Berger A. L. (1976) *Astron. Astrophys.*, 51, 127–135. [18] Ward W. R. (1979) *JGR*, 84, 237–241. [19] Laskar J. (1986) *Astron. Astrophys.*, 157, 59–70. [20] Hargreaves R. (1895) *Trans. Camb. Phil. Soc.*, 16, 58–94. [21] Milankovitch M. (1920) *Theorie Mathématique des Phénomènes Thermiques Produits par la Radiation Solaire*, Gauthier-Villars, Paris, 336 pp. [22] North G. R. and Coakley J. A. (1979) *J. Atmos. Sci.*, 36, 1189–1204. [23] Taylor K. E. (1984) In *Milankovitch and Climate* (A. L. Berger et al., eds.), 113–125, Reidel, Dordrecht. [24] Bills B. G. (1992) *Clim. Dynam.*, submitted. [25] Laskar J. et al. (1992) *Icarus*, 95, 148–152. [26] Cazenave A. and Daillet S. (1981) *JGR*, 86, 1659–1663. [27] Christodoulidis D. C. et al. (1988) *JGR*, 93, 6216–6236. [28] Berger et al. (1989) *Paleocean*, 4, 555–564. [29] Hansen K. S. (1982) *Rev. Geophys. Space Phys.*, 20, 457–480. [30] Platzman G. W. et al. (1981) *J. Phys. Ocean.*, 11, 579–603. [31] Dickman S. R. and Preisig J. R. (1986) *Geophys. J.*, 87, 295–304. [32] Olsen P. E. (1986) *Science*, 234, 842–848. [33] Williams G. E. (1989) *J. Geol. Soc. London*, 146, 97–111. [34] Williams G. E. (1989) *Eos*, 70, 33–41. [35] Herbert T. D. and D'Hondt S. L. (1990) *EPSL*, 99, 263–275. [36] Thomson D. J. (1990) *Trans. R. Soc. Lond.*, A332, 539–597. [37] Le Treut H. and Ghil M. (1983) *JGR*, 88, 5167–5190. [38] Wu P. and Peltier W. R. (1984) *Geophys. J.*, 76, 753–791. [39] Nakiboglu S. M. (1982) *PEPI*, 28, 302–311. [40] Smith M. L. and Dahlen A. F. (1981) *Geophys. J.*, 64, 223–281. [41] Stacey F. D. (1973) *Geophys. J.*, 33, 47–55. [42] Poincare H. (1910) *Bull. Astron.*, 27, 322–356. [43] Toomre A. (1966) In *The Earth-Moon System*, 33–45, Plenum. [44] Voorhies C. V. (1991) *J. Geomag. Geoelec.*, 43, 131–156. [45] Merriam J. B. (1988) *PEPI*, 50, 280–290. [46] Smylie D. E. et al. (1990) *Geophys. J. Int.*, 100, 183–192. [47] Wu P. (1990) *Geophys. J. Int.*, 101, 213–231. [48] Rochester M. G. (1962) *JGR*, 67, 4833–4836. [49] Sasao T. et al. (1977) *Publ. Astron. Soc. Japan*, 29, 83–105. [50] Kubo Y. (1979) *Celest. Mech.*, 19, 215–241. [51] Goldreich P. and Peale S. J. (1970) *Astron. J.*, 75, 273–284. [52] Ward W. R. and DeCampi W. M. (1979) *Astrophys. J. Lett.*, 230, 117–121. [53] Bills B. G. (1990) *LPSC XXI*, 81–82.

N93-19804P13

CONDENSATION PHASE OF THE MARTIAN SOUTH POLAR CAP. J. Capuano, M. Reed, and P. B. James, Department of Physics and Astronomy, University of Toledo, Toledo OH 43606, USA.

One type of database that can be useful in constraining models of the martian surface-atmosphere system is the time-dependent boundary of CO₂ frost for the polar caps. These

data have the advantage of spanning a large number of annual cycles on the planet, although, because a large fraction of the coverage is Earth based, the resolution for interannual comparisons is somewhat limited.

A more significant problem with these data is that they are almost exclusively obtained during the spring-summer recessions of the two polar caps. There are good reasons for this heavy weighting toward the sublimation phases, especially in the telescopic data. The martian poles are tilted away from the Sun, and therefore from Earth, between the fall and spring equinoxes. The presumed edge of the polar cap during fall and winter therefore barely extends past the terminator, where the resolution is degraded both by geometry and by the martian atmosphere. An additional complication is clouds, especially in the north polar region where the edge of the cap is obscured by the polar hood throughout most of the deposition seasons. The same lighting and obscuration problems are also a problem for spacecraft observations, though to a much smaller degree; however, there are few observations of the fall-winter caps in the set of spacecraft observations.

Data acquired by thermal infrared sensors on spacecraft are not constrained by the lighting problems that hamper visual observations. The surface temperature of solid CO_2 is constrained by Clapeyron's Equation as a function of the local partial pressure of CO_2 gas. The latter depends on the elevation, scale height, and total amount of CO_2 that is condensed in both polar regions; however, the temperature varies relatively slowly with pressure and, assuming that the surface temperature for polar CO_2 deposits is constant at some T between 147 and 150 K, is a valid first approximation. The infrared data are, however, potentially susceptible to deviations of the frost from blackbody conditions as well as to optically thick clouds, which can suppress the observed temperature through scattering.

We have investigated the growth of the martian south polar cap using the Viking IRTM dataset, which is available on the Atmospheres Node of the Planetary Data System in Boulder, Colorado. These data are available in five bands, four of which should correspond to surface radiation in clear conditions; we have chosen to work with the 20- μm data in the first phases of the project. The data are binned in 2° latitude and longitude intervals, in 10° intervals of areocentric solar longitude, L_s , and in 4-hr intervals of the local time of day at which the observations were made. We chose here to average over the local time variable; this is justified by the fact that many of the models do not include diurnal effects in predicting cap edges and by the fact that the diurnal effects should be small compared to the bin size. The effects of this averaging will be considered at a later time. We have also divided the data into three longitude bins: 1-45, 170-220, and 300-345. These were chosen because the extensive Viking dataset pertaining to south polar regression shows very different temporal and spatial behaviors in these three regions [1]. It is hoped that some

correlation with the behavior during condensation may be found to help explain the large south polar cap asymmetry.

The major deficiency of these data is that they are binned in $10^\circ L_s$ increments so that the temporal resolution is not very desirable. In addition, there are no data for some of the regions of interest in some of these time bins. However, we have been able to extract "curves of growth" for the three cap wedges mentioned above, which are shown in Fig. 1. There are some anomalous time periods in particular regions in which the "curves of growth" appear to be discontinuous; the most obvious one occurs between 330° and 45° longitude and between $L_s = 45$ and 55. This anomalous behavior shows up in all the wavelength bands that will respond to the lower atmosphere and surface, so it therefore seems likely that this is a real effect rather than a data problem. The most likely explanation for such excursions appears to be that clouds near the edge of the cap are affecting the measured brightness temperatures by scattering the infrared radiation emitted by the surface; if the effect were due to a reduced emissivity for fresh CO_2 deposits it would be more likely to show up more often in the data. Clouds were identified as a likely mechanism for the very low temperatures observed in the polar regions during the Viking Mission [2] and are predicted by GCM simulations [3] under some conditions. After $L_s = 200^\circ$ the data points show the effects of dust storms on Mars that commenced at $L_s = 205^\circ$ and cannot be used straightforwardly.

The data points from early autumn define a relatively smooth "curve of growth" for the cap that seems to be consistent with the limited visual data available. There is some suggestion of a lag in cap growth between longitudes 170 and 220, which could be correlated with the early removal of frost in these regions during mid spring, though the statistical significance of the observed difference is not overwhelming. The peak in cap size seems to occur just before winter solstice, which is earlier than models suggest for the maximum

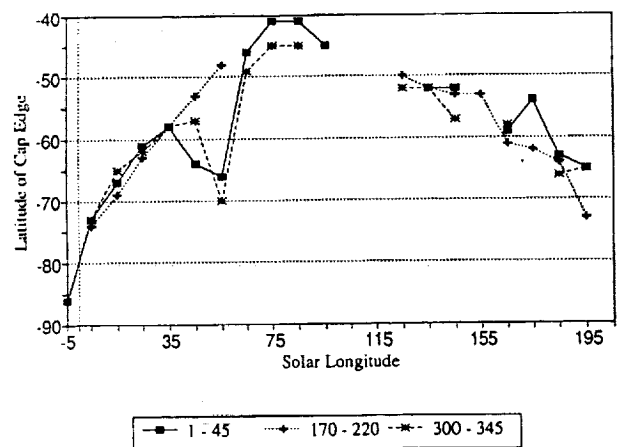


Fig. 1. South polar ice cap.

extent. It is possible that these bins could be dominated by data from the Argyre and Hellas Basins, which are within the two longitude wedges represented at these times; further study of the data in these L_s bins will be needed to resolve this question.

Acknowledgments: This work was partially supported by the NASA Planetary Atmospheres Program through Grant NAGW 2337.

References: [1] James P. B. et al. (1979) *JGR*, 84, 2889–2922. [2] Kieffer H. H. et al. (1976) *Science*, 193, 780–786. [3] Pollack J. B. et al. (1990) *JGR*, 95, 1447–1474.

N93-19805 P-2

WATER ON MARS: INVENTORY, DISTRIBUTION, AND POSSIBLE SOURCES OF POLAR ICE. S. M. Clifford, Lunar and Planetary Institute, 3600 Bay Area Blvd., Houston TX 77058, USA.

Theoretical considerations and various lines of morphologic evidence suggest that, in addition to the normal seasonal and climatic exchange of H_2O that occurs between the martian polar caps, atmosphere, and mid- to high-latitude regolith (e.g., [1,2]), large volumes of water have been introduced into the planet's long-term hydrologic cycle by the sublimation of equatorial ground ice, impacts, catastrophic flooding, and volcanism. Under the climatic conditions that are thought to have prevailed on Mars throughout the past 3–4 b.y., much of this water is expected to have been cold-trapped at the poles. In this abstract the amount of polar ice contributed by each of the planet's potential crustal sources is discussed and estimated. The final analysis suggests that only 5–15% of this potential inventory is now in residence at the poles.

Recent estimates of the inventory of water on Mars suggest that the planet has outgassed the equivalent of a global ocean at least several hundred meters deep. Evidence for such a large inventory is provided by a long list of martian landforms whose morphology has been attributed to the existence of subsurface volatiles [3–6]. In particular, it is supported by the existence of the martian outflow channels, whose distribution, size, and range of ages suggest that a significant body of groundwater was present on Mars throughout much of its geologic history [4,5,7,8]. Based on a conservative estimate of the discharge required to erode the channels, and the likely extent of their original source region, Carr [4,5] estimates that Mars may have outgassed the equivalent of a global ocean of water 0.5–1 km deep.

On Mars there are essentially three reservoirs in which water can reside: the atmosphere, perennial polar caps, and near-surface crust. Of these, the atmosphere is known to contain ~15 precipitable micrometers of water averaged over the planet's surface, while the quantity of water stored as ice in the polar caps is equivalent to a global layer approximately 10 m deep. This leaves more than 98% of the suspected

global inventory of water on Mars unaccounted for—virtually all of which is thought to reside as ground ice and groundwater beneath the surface.

Although mean annual surface temperatures are below freezing everywhere on Mars, observations made by the Viking Orbiter Mars Atmospheric Water Detectors (MAWD) indicate a globally averaged frost point temperature of ~198 K. Therefore, given the present latitudinal range of mean annual surface temperatures (~154–218 K), any subsurface H_2O is unstable with respect to the water vapor content of the atmosphere at latitudes equatorward of $\pm 40^\circ$ [9].

The survival of ground ice at equatorial and temperate latitudes was considered in detail by both Clifford and Hillel [10] and Fanale et al. [11]. They found that, for reasonable values of porosity and pore size, the near-equatorial crust has probably been desiccated to a depth of 300–500 m over the past 3.5 b.y., assuming that our present knowledge of the quasiperiodic changes in martian obliquity and orbital elements is accurate (e.g., [12–14]). However, because the sublimation of H_2O is sensitively dependent on temperature, the quantity of ice lost from the regolith is expected to decline with increasing latitude, falling to perhaps a few tens of meters at a latitude of 35° [10,11].

By integrating the the likely pore volume between the martian surface and the desiccation depths discussed above, Fanale et al. [11] have estimated that over the course of martian geologic history as much as $2.7\text{--}5.6 \times 10^6 \text{ km}^3$ of H_2O (equivalent to a global ocean ~20–40 m deep) may have been sublimated from the equatorial regolith and cold-trapped at the poles. However, as mentioned at the outset of this discussion, the sublimation of equatorial ground ice is just one of several potential processes that may have episodically introduced large volumes of water into the atmosphere.

Perhaps the clearest evidence that the martian crust has been a major source of atmospheric water are the outflow channels. The abrupt emergence of these features from regions of collapsed and disrupted terrain suggests that they were formed by a massive and catastrophic release of groundwater [7,8,15]. Channel ages, inferred from the density of superposed craters, indicate at least several episodes of flooding—the oldest dating back as far as the Late Hesperian (~2–3 b.y. ago), while the youngest may have formed as recently as the Mid-to-Late Amazonian (i.e., within the last 1 b.y.) [16–20]. Based on a conservative estimate of how much material was eroded to form the channels (~ $5 \times 10^6 \text{ km}^3$) and the maximum sediment load that the flood waters could have carried (40% by volume), Carr [5] has estimated a minimum cumulative channel discharge of $7.5 \times 10^6 \text{ km}^3$ of H_2O (the equivalent of a global ocean ~50 m deep).

Impacts into the ice-rich crust may have been another important source of atmospheric water. Assuming that the thickness of permafrost on Mars averages about 2.5 km and has an ice content of 20%, the volume of water excavated